ELSEVIER

Journal of Organometallic Chemistry 573 (1999) 237–246

Journal of Organometallic Chemistry

Cluster build-up reactions via the ionic coupling of tetraosmium anions and the $[RhCp^*(NCMe)_3]^{2+}$ cation; the crystal and molecular structures of $[Os_4Rh(\mu\text{-}H)_3(MeC{=}NH)(CO)_{11}(\eta^5\text{-}Cp^*)]$, $[Os_4Rh(\mu\text{-}H)_2(CO)_{13}(\eta^5\text{-}Cp^*)]$ and $[Os_4Rh_2(\mu\text{-}H)_2(CO)_{11}(\eta^5\text{-}Cp^*)_2]$ ($Cp^*{=}C_5Me_5$)[1]

William Clegg [b,c], Neil Feeder [a], Ana M. Martin Castro [a], Saifun Nahar [a], Paul R. Raithby [a,*], Gregory P. Shields [a], Simon J. Teat [b,c]

[a] *Department of Chemistry, University of Cambridge, Lensfield Road, Cambridge CB2 1EW, UK*
[b] *The Department of Chemistry of the University of Newcastle, Newcastle upon Tyne NE1 7RU, UK*
[c] *The CLRC Daresbury Laboratory, Warrington WA4 4AD, UK*

Received 6 April 1998; received in revised form 6 June 1998

Abstract

The reaction of $[Os_4H_4(CO)_{11}]^{2-}$ **2**, formed by the reduction of $[Os_4H_4(CO)_{12}]$ **1** with K/Ph_2CO, with the cation $[Rh(\eta^5\text{-}Cp^*)(MeCN)_3]^{2+}$ ($Cp^*{=}C_5Me_5$) **3**, affords a number of penta- and hexanuclear mixed-metal clusters depending on the reaction conditions. If only sufficient K/Ph_2CO is added to dissolve all of **1**, and the dication **3** added, a low yield of a blue cluster $[Os_4Rh(\mu\text{-}H)_3(MeC{=}NH)(CO)_{11}(\eta^5\text{-}Cp^*)]$ ($Cp^*{=}C_5Me_5$) **4** is obtained in addition to large quantities of **1**. If an excess of K/Ph_2CO is added so that reduction of **1** is complete, and then the dication **3** added, two new products $[Os_4Rh(\mu\text{-}H)_2(CO)_{13}(\eta^5\text{-}Cp^*)]$ **5** and $[Os_4Rh_2(\mu\text{-}H)_2(CO)_{11}(\eta^5\text{-}Cp^*)_2]$ **6** are obtained in low yield. The three new complexes have been characterised spectroscopically and crystallographically. Cluster **4** contains the uncommon MeC=NH group coordinated to an edge-bridged tetrahedral metal framework. The metal framework in **5** is also a Rh edge-bridged Os_4 tetrahedron while that of **6** is a bicapped tetrahedron, with two Rh atoms face capping two faces of an Os_4 tetrahedron.

Keywords: Osmium; Rhodium; Cluster; Cyclopentadienyl; Crystal structures

1. Introduction

The interest in the chemistry of high nuclearity transition metal cluster carbonyls has been maintained because of their potential use as models for heterogeneous catalysts [1], because of their ability to act as 'electron sinks', adopting a range of stable oxidation states [2], and because of their potential as precursors in quantum dot technology [3]. Johnson [4] and others [5] have developed systematic strategies to the synthesis of mixed-metal high nuclearity clusters using coupling reactions between lower nuclearity cluster carbonyl anions and mononuclear cation metal complexes. Johnson and coworkers [4] have recently shown that these mixed-metal clusters act as precursors for bimetallic nanoparticle catalysts that can be anchored inside mesoporous silica [6]. We have been interested in the mechanisms of the synthesis of mixed-metal clusters, and have embarked on a series of studies in order to identify the factors that are important in the cluster

* Corresponding author. Fax: +44 1223 336362; e-mail: prr1@cam.ac.uk

[1] Dedicated to Professor Brian Johnson on the occasion of his 60th birthday in recognition of his outstanding contribution to organometallic chemistry, and for his support and friendship over the years.

0022-328X/99/$ - see front matter
PII S0022-328X(98)00834-1

build-up processes and that determine the nature of the reaction products [7]. In this context mixed osmium–rhodium clusters are of particular interest because it has been shown recently that high nuclearity clusters such as $[Os_{12}Rh_9(CO)_{44}(\mu_3\text{-Cl})]$ can be formed by reaction of low nuclearity osmium cluster anions with neutral rhodium chloride complexes under relatively mild conditions [8]. We have investigated the capping reaction of the of the rhodium–containing cation $[Rh(\eta^5\text{-Cp*})(MeCN)_3]^{2+}$ **3,** that has previously been shown to form higher nuclearity clusters with osmium and ruthenium cluster anions [9,10], with anionic derivatives of the tetrahydrido–tetraosmium cluster $[Os_4H_4(CO)_{12}]$ **1**. By altering the reaction conditions for the reduction of **1**, we have isolated and characterised a series of new penta- and hexanuclear mixed Os/Rh cluster complexes including the cluster $[Os_4Rh(\mu\text{-H})_3(MeC{=}NH)(CO)_{11}(\eta^5\text{-Cp*})]$ **4** which may represent an intermediate in the reaction pathway.

2. Results and discussion

The tetrahydrido cluster $[Os_4H_4(CO)_{12}]$ **1** may be reduced with an excess of K/Ph_2CO, in THF, to produce the dianion $[Os_4H_4(CO)_{11}]^{2-}$ **2** [11]. The reaction of the dianion **2** with an excess of the dication $[Rh(\eta^5\text{-Cp*})(MeCN)_3]^{2+}$ (Cp*=C_5Me_5) **3**, as its $[BF_4]^-$ salt, in dichloromethane, was then carried out at r.t. The reaction proceeded rapidly as evidenced by an immediate colour change from orange/yellow to blue/violet, and three new products **4**–**6** were isolated in addition to quantities of the unreacted starting material, **1**. The yield of the products **4**–**6** was dependent on the amount of the reducing agent K/Ph_2CO added to the initial reaction. This observation led us to investigate the nature of the reaction in more detail.

In the first experiment only sufficient K/Ph_2CO was added to cluster **1**, so that it just dissolved, it being sparingly soluble in THF, and there was little change in the solution IR spectrum from that observed for **1**. An excess of the dication **3** was added at this point, and the new product **4** was obtained in low yield (ca. 2%) together with large quantities of the starting material **1**. Clearly, the reduction of **1** was incomplete, but the blue/violet cluster could be isolated and purified by thin layer chromatography (TLC). The complex was initially characterised by IR and NMR spectroscopy, mass spectrometry, and microanalysis (Table 1).

The positive ion FAB mass spectrum of **4** exhibited an intense molecular ion peak consistent with the formula $C_{26}H_{25}NO_{11}Os_4Rh$, and another strong peak corresponding to the loss of '$MeCNH_2$' from the molecule. Peaks corresponding to the subsequent, sequential loss of carbonyl ligands were also observed. The IR spectrum in the carbonyl region showed only peaks consistent with the presence of terminal carbonyl ligands, and a weak signal at 2927 cm^{-1} in the N–H stretching region was also observed. The r.t. ^{1}H-NMR spectrum was informative. A weak, broad peak was observed at δ 7.81 which could be attributed to an N–H proton. Two further peaks in the spectrum corresponding to the methyl protons of the η^5-C_5Me_5 and the MeCNH ligands were observed at δ 1.34 and 2.59, in a 5:1 ratio, respectively. Two peaks in the bridging hydride region, in a ratio of 1:2, were also observed at δ −17.7 and −18.0, consistent with two of the three hydrides occupying equivalent positions on the metal framework. The hydrides did not appear to be undergoing a fluxional process at this temperature. The low solubility of **4** prevented meaningful ^{13}C-NMR spectra from being obtained.

The spectroscopic characterisation of **4** showed that the Rh(η^5-Cp*) fragment was attached to the Os_4 cluster, but also suggested that one or more of the acetonitrile ligands, or a ligand derived from it, from the original cation **3** might also be present in the new cluster. In order to confirm this, and establish the geometry of the cluster a single-crystal X-ray analysis was carried out on crystals of **4** obtained by slow crystallisation from a dichloromethane–benzene solution. The molecular structure of $[Os_4Rh(\mu\text{-H})_3(MeC{=}NH)(CO)_{11}(\eta^5\text{-Cp*})]$ **4** is shown in Fig. 1 while selected bond parameters are listed in Table 2.

Table 1
Spectroscopic data for the new clusters **4**–**6**

Compound	IR (ν_{CO}/cm^{-1}) hexane[a], CH_2Cl_2[b]	^{1}H-NMR (δ) $CDCl_3$	^{13}C-NMR (δ) $CDCl_3$	FAB MS obs (Calc. ^{190}Os, ^{103}Rh)
4	2084w, 2077m, 2067m, 2041 m, 2022vs, 1998w, 1985vw, 1932vw[a]	7.81 (s, 1*H*, MeCN*H*); 1.34 (s, 15*H*, *Cp**); 2.59 (s, 3*H*, *Me*CNH); −17.7 (s, 1*H*); −18.0 (s, 2*H*)	—	1354 (1351)
5	2081s, 2065vw, 2047s, 2027vs, 2008vw[b]	1.57 (s, 15*H*, *Cp**); −18.7 (s, 1*H*); −20.5 (s, 1*H*)	97.65 (d, 5*C*, J_{Rh-C}, 7.8 Hz); 10.1 (s, 5*C*,*Cp**)	1367 (1364)
6	2034s, 2004m, 1990vs, 1924w, 1711vw[b]	1.54 (s, 30*H*,*Cp**); −7.12 (d, 2*H*, J_{Rh-H}, 13.1 Hz)	196.8 (s, 11*C*, *C*O); 97.2 (d, 10*C*, J_{Rh-C}, 7.3 Hz); 10.2 (s, 10*C*, *Cp**)	1548 (1546)

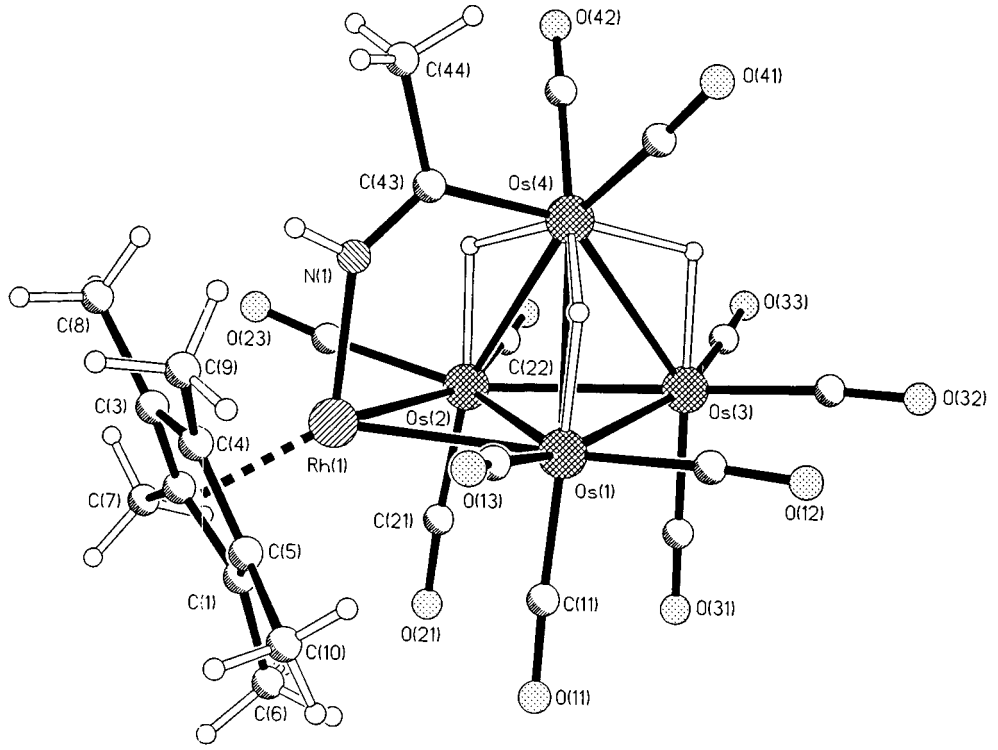

Fig. 1. The molecular structure of $[Os_4Rh(\mu\text{-}H)_3(MeC{=}NH)(CO)_{11}(\eta^5\text{-}Cp^*)]$ **4** showing the atom numbering scheme.

The metal framework in **4** consists of a tetrahedron of Os atoms, one edge of which is bridged by the Rh atom which is coordinated to the η^5-pentamethyl cyclopentadienyl ring. The 11 carbonyl groups are essentially linear and terminal, with three coordinated to each of Os(1), Os(2) and Os(3), and two coordinated to Os(4). The hydrides, which were located by potential energy calculations [12], bridge the three Os–Os edges associated with Os(4) to give the same arrangement as found for the C_{3v} isomer of the anions $[M_4H_3(CO)_{12}]^-$ (M = Ru, Os) [13]. This structure is consistent with the ^{1}H-NMR data for **4**. The most interesting feature of the structure is the 'MeC=NH' ligand which spans the 'wing tips' of the Os(1), Os(2), Os(4), Rh(1) butterfly fragment of the edge-bridged metal core. The nitrile ligand coordinates to Os(4) through C(43) and to Rh(1) through N(1). It is presumably derived from one of the acetonitrile ligands that was associated to the $[Rh(\eta^5\text{-}Cp^*)(MeCN)_3]^{2+}$ **3** cation, and has become involved in the coupling process between the cation and the cluster anion. The bond between the N atom and the Rh is retained, and a new bond has formed between a C atom and an Os atom. The hydrogen now bonded to N(1) may have migrated from the Os_4 core during the process. This nitrile ligand, or closely related species, have been observed previously in the cluster complexes $[Os_3H(\mu,\eta^2\text{-}(CF_3C{=}NH)(CO)_9PMe_2Ph]$ [14] and $[Fe_3H(CH_3C{=}NH)(CO)_9]$ [15] where the ligand bridges the edge of a metal triangle. The N(1)–C(43) bond length in **4** is similar in length to the values of 1.31(1) and 1.344(2) Å reported for the triosmium and triiron clusters, respectively, and is consistent with double bond character for this interaction.

The Rh(1) atom bridges the Os(1)–Os(2) edge symmetrically, and the Os–Rh distances are slightly longer than the values of 2.770(1) and 2.789(1) Å found in the related pentanuclear cluster $[Os_4Rh(\mu\text{-}H)_2(CO)_{13}(\eta^5\text{-}C_5H_5)]$ [16]. The presence of the MeC=NH ligand may

Table 2
Selected bond lengths (Å) and angles (°) for $[Os_4Rh(\mu\text{-}H)_3(MeC{=}NH)(CO)_{11}(\eta^5\text{-}Cp^*)]$ **4**

Os(1)–Os(2)	2.786(2)	Os(2)–Rh(1)	2.819(3)
Os(1)–Os(3)	2.840(2)	Rh(1)–Cp*(centroid)	2.186
Os(1)–Os(4)	2.964(2)	Rh(1)–N(1)	2.08(2)
Os(2)–Os(3)	2.834(2)	Os(4)–C(43)	2.00(3)
Os(2)–Os(4)	2.959(2)	C(43)–C(44)	1.59(4)
Os(3)–Os(4)	2.983(2)	N(1)–C(43)	1.26(3)
Os(1)–Rh(1)	2.814(3)		
N(1)–Rh(1)–Os(1)	89.1(6)	N(1)–C(43)–Os(4)	125(2)
N(1)–Rh(1)–Os(2)	89.3(5)	Os(4)–C(43)–C(44)	121(2)
C(43)–N(1)–Rh(1)	135(2)	C(43)–Os(4)–Os(1)	91.1(7)
N(1)–C(43)–C(44)	115(2)	C(43)–Os(4)–Os(2)	91.7(7)

have an influence on these bond parameters, as it does on the dihedral angles around this part of the metal skeleton. The dihedral angle between the Os(1)Os(2)Rh(1) and the Os(1)Os(2)Os(4) planes is 80.0°, while that between the Os(1)Os(2)Rh(1) and Os(1)Os(2)Os(3) planes is 8.2°. The Os(1)–Os(2) edge that is bridged by the Rh(1) atom is the shortest Os–Os contact in the structure, a feature that is in keeping with several pentaosmium clusters which adopt the edge bridged tetrahedral geometry [17]. The three longest edges in the osmium framework are those which are bridged by the hydride ligands, as is observed in the related anion $[Os_4H_3(CO)_{12}]^-$ [13]. If the nitrile ligand acts as a three electron donor, then the electron count for the molecule is 74 electrons, which is consistent with the edge-bridged tetrahedral metal framework.

Once the structure of **4** had been established and had been shown to contain a ligand derived from an acetonitrile group in the starting material, it was appealing to consider this complex as an intermediate in the production of new, higher nuclearity clusters. In subsequent experiments sufficient quantities of the reducing agent K/Ph_2CO were added to the suspension of **1** for complete reduction to occur, as indicated by changes in the IR spectrum which showed the disappearance of peaks corresponding to **1** and the appearance of those corresponding to **2**. The addition of **3** to the solution of **2** and subsequent work up and purification as described above afforded the two new clusters **5** (10% yield) and **6** (2% yield), together with quantities of **1**. The yield of **6** could be improved, to 12%, by adding a further excess of K/Ph_2CO in the initial reduction of **1**.

The products **5** and **6** were initially characterised by IR and NMR spectroscopy, and by mass spectrometry (Table 1). The positive ion FAB mass spectrum of **5** showed a molecular ion peak at m/z 1367 which is in good agreement with the formulation $[Os_4Rh(\mu\text{-}H)_2(CO)_{13}(\eta^5\text{-}Cp^*)]$, and the IR spectrum in the carbonyl region showed the presence of only terminal carbonyl ligands, the band pattern being quite similar to that reported for $[Os_4Rh(\mu\text{-}H)_2(CO)_{13}(\eta^5\text{-}Cp)]$ [16]. In the ^{1}H-NMR spectrum, at r.t., the characteristic peak for the η^5-Cp* ligand is found at δ 1.57 which is 0.23 ppm downfield to that found for complex **4**. Two further resonances are observed at δ −18.7 and −20.5, in the bridging hydride region of the spectrum, with an intensity ratio of 1:3. These resonances remained unchanged on cooling the sample from 295 to 233 K, which is consistent with the presence of two non-interconverting isomers (on the NMR timescale), which were inseparable by TLC. The major isomer is thought to have two equivalent bridging hydrides, consistent with the solid state structure (vide infra), while the minor isomer has two inequivalent hydrides, one of them occupying the same position as in the major isomer. The ^{13}C-NMR spectrum of **5** exhibits a singlet resonance at δ 10.1 and a doublet centred at $\boldsymbol{\delta}$ 97.65 ($J_{Rh-C} = 7.8$ Hz) corresponding to the methyl and ring carbons of the η^5-Cp* ligand. The splitting of the cyclopentadienyl carbon signal by the ^{103}Rh nucleus is consistent with that observed for other cluster complexes that contain the $Rh(\eta^5\text{-}Cp^*)$ unit [18]. Signals corresponding to the carbonyl ligands were not observed, perhaps because of the relatively low solubility of the cluster.

For cluster **6** the molecular ion in the mass spectrum is consistent with the molecular formulation as $[Os_4Rh_2(\mu\text{-}H)_2(CO)_{11}(\eta^5\text{-}Cp^*)_2]$, while the IR spectrum indicates that both terminal and edge bridging carbonyls are present in the structure. The ^{1}H-NMR spectrum shows only one peak in the region corresponding to the methyl protons of the η^5-Cp* group, at δ 1.54, in a similar position to that found for the methyl protons in **5**. This suggests that the two $Rh(\eta^5\text{-}Cp^*)$ groups are in equivalent environments in the cluster, and this is borne out by the ^{13}C-NMR spectrum which exhibits only one singlet at δ 10.2 that can be assigned to the methyl carbons and one doublet at δ 97.2 ($J_{Rh-C} = 7.3$ Hz) that can be assigned to the cyclopentadienyl carbons split by the ^{103}Rh nucleus. The ^{1}H-NMR spectrum also exhibits a doublet in the hydride region, at δ −7.12 with $J_{Rh-H} = 13.1$ Hz, indicating that each of the equivalent edge bridging hydrides couples to a ^{103}Rh nucleus. This coupling constant is in good agreement with the value of $J_{Rh-H} = 13.5$ Hz found for the hydride that is directly bonded to the Rh nucleus in $[Ru_3RhH_4(CO)_9(\eta^5\text{-}Cp^*)]$ [19]. A single ^{13}CO resonance is observed at δ 196.8 in the ^{13}C-NMR spectrum which suggests that all the carbonyl groups in the cluster are involved in a rapid exchange process at r.t.

In order to confirm the spectroscopic assignments and establish the molecular structures of **5** and **6** single-crystal X-ray diffraction studies were undertaken on both compounds. The molecular structure of $[Os_4Rh(\mu\text{-}H)_2(CO)_{13}(\eta^5\text{-}Cp^*)]$ **5** is shown in Fig. 2 while selected bond parameters are listed in Table 3. The molecule sits on a crystallographic mirror plane which passes through Os(1), Os(2), Rh(4), C(12), O(12), C(14), O(14), C(5) and C(51). The metal core consists of a tetrahedron of osmium atoms with a $Rh(\eta^5\text{-}Cp^*)$ group bridging one edge to produce the edge bridged tetrahedral geometry observed for **4**. However, the absence of the bridging nitrile ligand, which was present in **4**, causes changes in the dihedral angles between the edge bridging unit and the central tetrahedron. In **5** the dihedral angle between the Os(3)Os(3a)Rh(4) and the Os(2)Os(3)Os(3a) planes is 61.4° and that between Os(3)Os(3a)Rh(4) and Os(1)Os(3)Os(3a) is 5.3°, compared to equivalent values of 80.0° and 8.2° for **4**. The overall geometry of **5** is similar to that of the cyclopentadiene analogue $[Os_4Rh(\mu\text{-}H)_2(CO)_{13}(\eta^5\text{-}Cp)]$ [16] that has been characterised previously. The metal–metal

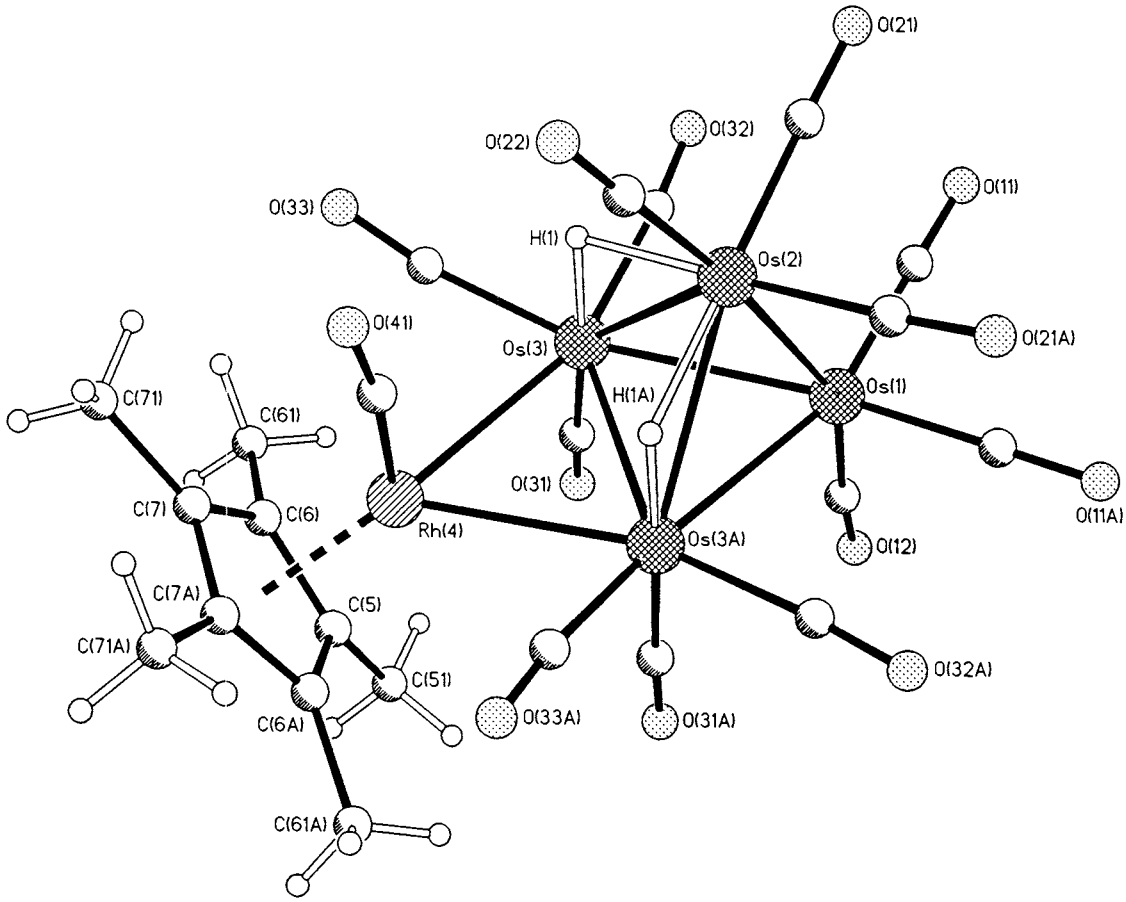

Fig. 2. The molecular structure of $[Os_4Rh(\mu\text{-}H)_2(CO)_{13}(\eta^5\text{-}Cp^*)]$ **5** showing the atom numbering scheme.

bond lengths follow the same trends with the shortest Os–Os bond in the structures being that bridged by the Rh(η^5-cyclopentadienyl) groups and the two longest those bridged by the hydrides; in **5** the positions of the hydrides were obtained from potential energy calculations [12]. In **5** the Rh(4) atom is required to bridge symmetrically by crystallographic symmetry, and the Rh(4)–Os(3/3a) distance is ca. 0.02 Å longer than the average of the two Rh–Os distances (2.78 Å) in $[Os_4Rh(\mu\text{-}H)_2(CO)_{13}(\eta^5\text{-}Cp)]$ [16], but very similar to the average value of 2.817 Å for the Rh–Os bonds in **4**. In terms of electron counting, the cluster has a count of 74 electrons which is consistent with the edge bridged tetrahedral metal framework.

The molecular structure of $[Os_4Rh_2(\mu\text{-}H)_2(CO)_{11}(\eta^5\text{-}Cp^*)_2]$ **6** is shown in Fig. 3 and selected bond parameters are listed in Table 4. The metal framework is based on a central Os_4 tetrahedron with two Rh(η^5-Cp*)

Table 3
Selected bond lengths (Å) and angles (°) for $[Os_4Rh(\mu\text{-}H)_2(CO)_{13}(\eta^5\text{-}Cp^*)]$ **5**

Os(1)–Os(2)	2.7856(5)	Os(1)–Os(3)	2.8278(4)
Os(2)–Os(3)	2.9451(4)	Os(3)–Os(3a)	2.7707(5)
Os(3)–Rh(4)	2.8129(6)	Rh(4)–C(41)	1.850(10)
C(41)–O(41)	1.163(12)	Os–C(mean)	1.915
C–O(mean)	1.15	Rh–Cp*(centroid)	2.251
Os(1)–Os(2)–Os(3)	59.056(10)	Os(1)–Os(3)–Os(2)	57.660(11)
Os(2)–Os(1)–Os(3)	63.284(10)	Rh(4)–Os(3)–Os(2)	97.82(2)
Rh(4)–Os(3)–Os(1)	120.944(12)	Os(3)–Os(1)–Os(3a)	58.669(12)
Os(3)–Os(2)–Os(3a)	56.120(12)	Os(3)–Rh(4)–Os(3a)	59.01(2)
Os(3a)–Os(3)–Os(1)	60.666(6)	Os(3a)–Os(3)–Os(2)	61.940(6)
Os(3a)–Os(3)–Rh(4)	60.495(8)		

Symmetry transformation used to generate equivalent atoms denotes 'a' is x, $0.5-y$, z.

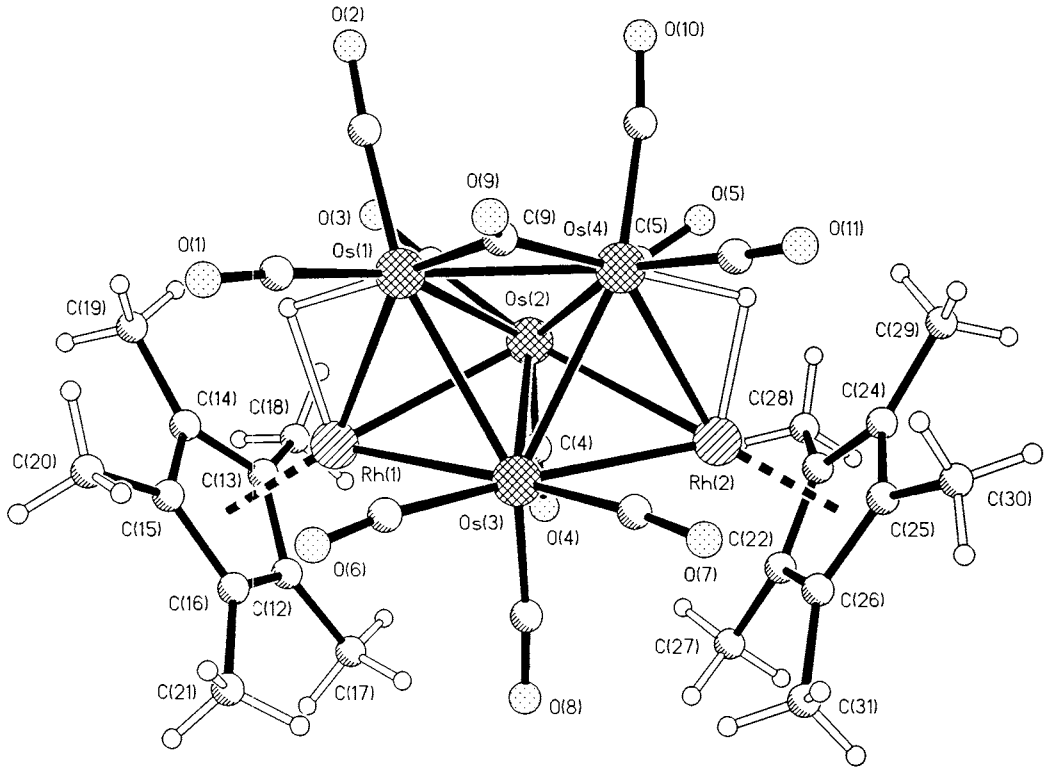

Fig. 3. The molecular structure of $[Os_4Rh_2(\mu\text{-}H)_2(CO)_{11}(\eta^5\text{-}Cp^*)_2]$ **6** showing the atom numbering scheme.

fragments capping the Os(1)Os(2)Os(3) and Os(2)Os(3)Os(4) faces. The two hydrides, the positions of which were established by potential energy calculations [12], bridge the Os(1)–Rh(1) and Os(4)–Rh(2) edges. Ten of the carbonyl groups are terminal and essentially linear while the eleventh bridges the Os(1)–Os(4) edge. Complex **6** is an 84 electron system, and is isoelectronic with the parent binary carbonyl, $[Os_6(CO)_{18}]$ [20], which also exhibits the bicapped tetrahedral geometry. The metal core geometry in **6** and in $[Os_6(CO)_{18}]$ could also be described as a capped trigonal bipyramid if using the polyhedral skeletal electron pair method of electron counting, the two descriptions are equivalent. Although the metal–metal bonding in clusters is certainly delocalised in character, it is sometimes helpful when interpreting the chemistry to consider a more localised approach to the bonding; this is the case when interpreting the structure of cluster **6**. In simplistic terms, within the bicapped tetrahedral framework, there are three different metal environments. The capping metals, Rh(1) and Rh(2), in this case, form three metal–metal contacts, and have a formal count of 17 electrons; the Os(1) and Os(4) atoms have four metal–metal contacts and a formal electron count of 18 electrons; the Os(2) and Os(3) atoms have five metal–metal contacts and a formal electron count of 19 electrons. It is interesting to note that in this hydrido cluster **6** the two $Rh(\eta^5\text{-}Cp^*)$ fragments occupy the two capping, 17 electron sites, although they are considered to be much better donor groups to the metal core than $Os(CO)_3$ fragments, and might therefore be expected to occupy the formally 'electron rich' 19 electron centres. In fact in the related cluster $[Ru_5Rh(CO)_{12}(\mu\text{-}CO)(\mu_4\text{-}\eta^2\text{-}CO)_2(\eta^5\text{-}Cp^*)]$ [10] the $Rh(\eta^5\text{-}Cp^*)$ fragment does occupy a 19 electron site, and, perhaps, as a result of the steric crowding, the cluster opens out to form the bis–edge bridged tetrahedral core with the two novel $\mu_4\text{-}\eta^2$-CO ligands. Also in contrast to **6** the benzene capped metal cluster $[Os_6(CO)_{12}(\eta^6\text{-}C_6H_6)_2]$ [21] in which there are two $Os(\eta^6\text{-}C_6H_6)$ fragments displays a geometry in which one $Os(\eta^6\text{-}C_6H_6)$ fragment occupies a 17 electron capping site and the other an 18 electron site. The $Os(\eta^6\text{-}C_6H_6)$ fragment is considered not to be either as sterically demanding as the $Rh(\eta^5\text{-}Cp^*)$ fragment nor to be such a good donor group, so that the ligand arrangement in $[Os_6(CO)_{12}(\eta^6\text{-}C_6H_6)_2]$ is easier to rationalise. This variation in occupancy of the different metal sites by the arene groups is considered to be a balance between steric and electronic factors [7]. The electronic factors, which as indicated above may be related to the enhanced donor power of the metal arene fragment, compared to a metal carbonyl fragment, would favour substitution in the order of metal–metal connectivity five > four > three, whereas steric factors would favour the reverse order. The capping positions are the least sterically crowded in the bicapped tetrahedral geometry, and these are the positions of the $Rh(\eta^5\text{-}Cp^*)$ fragments in **6**, so that steric factors may dominate over electronic when two $Rh(\eta^5\text{-}Cp^*)$ fragments are involved.

The Os–Os distances in **6** follow the same trends as within the central tetrahedron of $[Os_6(CO)_{18}]$ [20], with the shortest contact between the two 18 electron centres and the longest between the pairs of 18 and 19 electron centres. However, the Os(1)–Os(4) distance in **6** is 0.09 Å shorter than the equivalent bond in $[Os_6(CO)_{18}]$ (2.732(1) Å), and is bridged by a carbonyl ligand. The edge shortening effect of a bridging carbonyl has been observed in a number of metal arene clusters [21,22], but the bridge is usually directly associated with the metal bearing the arene ligand; this in not the case in **6**. The Rh atoms cap the two triangular Os faces asymmetrically, but the hydride bridged Os–Rh edges are not the longest, and in fact there is little difference between the hydride bridged edge and one of the other edges. The longest Os–Rh edges both involve Os(2) and are closest to being *trans* to the cyclopentadienyl groups.

These results, and the characterisation of the three products **4**, **5** and **6**, do indicate that the conditions of the reduction of **1** with K/Ph_2CO are important in determining which reaction products are obtained. The isolation of $[Os_4Rh(\mu\text{-}H)_3(MeC{=}NH)(CO)_{11}(\eta^5\text{-}Cp^*)]$ **4** is of interest, and potentially this product could be viewed as an intermediate in the formation of **5** and **6**. Unfortunately, it has not been possible to isolate sufficient quantities of **4** to carry out reaction chemistry and establish whether or not it is indeed the intermediate. However, it is probable that in the formation of **4**, the cation **3** loses two of its acetonitrile ligands and one hydrogen from the cluster anion **2** is transferred to the remaining acetonitrile ligand. The second product $[Os_4Rh(\mu\text{-}H)_2(CO)_{13}(\eta^5\text{-}Cp^*)]$ **5** could be formed from **4** by cleavage of the Rh–N and C(43)–Os(4) bonds while two carbonyl ligands could be scavanged from the reaction mixture. The elimination of the nitrile group 'CH_3CNH_2' from **4** may be facilitated by abstraction of another hydride from the bridged metal centres. The structures of **4** and **5** suggest that the additional two carbonyl groups in **5** are connected to those metal atoms which were initially bridged by the CH_3CNH_2 group in **4**. Addition of excess reducing agent to **5** could eliminate further carbonyl groups and form the dianion '$[Os_4RhH_2(CO)_{11}Cp^*]^{2-}$' that could then add another cationic '$[RhCp^*]^{2+}$' and produce the hexanuclear cluster $[Os_4Rh_2(\mu\text{–}H)_2(CO)_{11}(\eta^5\text{-}Cp^*)_2]$ **6**.

Table 4
Selected bond lengths (Å) and angles (°) for $[Os_4Rh_2(\mu\text{-}H)_2(CO)_{11}(\eta^5\text{-}Cp^*)_2]$ **6**

Os(1)–Os(2)	2.828(2)	Os(3)–Rh(1)	2.766(2)
Os(1)–Os(3)	2.839(2)	Os(2)–Rh(2)	2.850(2)
Os(1)–Os(4)	2.6422(14)	Os(3)–Rh(2)	2.748(2)
Os(2)–Os(3)	2.7461(14)	Os(4)–Rh(2)	2.789(2)
Os(2)–Os(4)	2.804(2)	Os(1)–C(9)	2.14(3)
Os(3)–Os(4)	2.835(2)	Os(4)–C(9)	2.09(3)
Os(1)–Rh(1)	2.766(3)	C(9)–O(9)	1.13(3)
Os(2)–Rh(1)	2.858(2)		
Os(4)–Os(1)–Os(2)	61.57(5)	Rh(1)–Os(3)–Os(4)	107.13(6)
Os(4)–Os(1)–Os(3)	62.18(5)	Rh(2)–Os(3)–Os(1)	108.19(5)
Rh(1)–Os(1)–Os(2)	61.45(5)	Os(2)–Os(3)–Os(1)	60.80(4)
Rh(1)–Os(1)–Os(3)	59.12(5)	Rh(1)–Os(3)–Os(1)	59.12(6)
Os(2)–Os(1)–Os(3)	57.97(3)	Os(4)–Os(3)–Os(1)	55.50(3)
Os(4)–Os(1)–Rh(1)	112.86(6)	Os(1)–Os(4)–Rh(2)	112.83(7)
Os(3)–Os(2)–Os(4)	61.43(4)	Rh(2)–Os(4)–Os(2)	61.27(6)
Os(4)–Os(2)–Os(1)	55.96(3)	Os(1)–Os(4)–Os(3)	62.32(4)
Os(4)–Os(2)–Rh(2)	59.11(4)	Os(2)–Os(4)–Os(3)	58.28(5)
Os(3)–Os(2)–Rh(2)	58.77(5)	Os(1)–Os(4)–Os(2)	62.47(4)
Os(4)–Os(2)–Rh(1)	105.47(6)	Rh(2)–Os(4)–Os(3)	58.48(6)
Os(1)–Os(2)–Rh(2)	105.70(5)	Os(1)–Rh(1)–Os(2)	60.34(5)
Os(1)–Os(2)–Rh(1)	58.21(6)	Os(3)–Rh(1)–Os(2)	58.43(4)
Rh(2)–Os(2)–Rh(1)	114.43(5)	Os(3)–Rh(2)–Os(4)	61.60(5)
Os(2)–Os(3)–Rh(2)	62.51(5)	Os(3)–Rh(2)–Os(2)	58.72(4)
Rh(2)–Os(3)–Rh(1)	121.02(6)	Os(4)–Rh(2)–Os(2)	59.62(5)
Os(2)–Os(3)–Rh(1)	62.47(5)	Os(4)–C(9)–Os(1)	77.3(10)
Os(2)–Os(3)–Os(4)	62.29(3)	Os(4)–C(9)–O(9)	142(2)
Rh(2)–Os(3)–Os(4)	59.92(4)	O(9)–C(9)–Os(1)	140(2)

3. Experimental

All the reactions were performed under an atmosphere of dry, oxygen-free nitrogen using standard schlenk techniques. Technical grade solvents were purified by distillation over the appropriate drying agents and under an inert nitrogen atmosphere prior to use. Routine separation of products was performed by TLC, using commercially prepared glass plates, precoated to 0.25 mm thickness with Merck Kieselgel 60 F_{254}, as supplied by Merck, or using laboratory prepared glass plates coated to 1 mm thickness with Merck Kieselgel 60 F_{254}. The complexes $[Os_4H_4(CO)_{12}]$ [23], $K_2[Os_4H_4(CO)_{11}]$ [24] and $[Rh(\eta^5\text{-}Cp^*)(MeCN)_3][BF_4]_2$ [25] were prepared by literature procedures. FAB Mass spectra were recorded using a Kratos model MS 902. IR spectra were recorded on a Perkin-Elmer 1710 FT-IR spectrometer, using 0.5 mm NaCl or CaF_2 cells, and ^1H- and ^{13}C-NMR spectra on a Bruker WH 250 MHz spectrometer.

3.1. Preparation of $K_2[Os_4H_4(CO)_{11}]$ 2 [24]

In a typical reaction, a freshly prepared solution of K/Ph_2CO in THF was added dropwise to a suspension of $[Os_4H_4(CO)_{12}]$ **1** (50 mg, 0.045 mmol), in THF, until all the material dissolved. The resulting orange solution gave a highly air-sensitive dianion $[Os_4H_4(CO)_{11}]^{2-}$ **2** which was identified by comparison with the reported IR spectrum [24]. After removal of solvent, the remaining orange/brown residue was used without further purification. IR (ν_{CO}/cm^{-1}, THF): 2047w, 1968s, 1923w.

Table 5
Crystal data and structure solution and refinement parameters for compounds **4**, **5** and **6**[a]

Complex	**4**	**5**	**6**
Molecular formula	$C_{23}H_{22}NO_{11}Os_4Rh \cdot 0.5C_6H_6$	$C_{23}H_{17}O_{13}Os_4Rh$	$C_{31}H_{32}O_{11}Os_4Rh_2$
Formula weight	1391.18	1365.08	1547.19
Temperature (K)	150(2)	160(2)	150(2)
Wavelength of radiation (Å)	0.71073	0.6956	0.71069
Crystal system	Monoclinic	Orthorhombic	Orthorhombic
Space group	$P2_1/c$	*Pnma*	$Pca2_1$
Unit cell dimensions			
a (Å)	13.443(7)	17.9824(9)	16.979(8)
b (Å)	19.970(10)	13.8490(7)	11.997(6)
c (Å)	13.266(7)	11.5678(6)	17.69(2)
β (°)	119.59(3)	90.00	90.00
U (Å^3)	3097(3)	2880.8(3)	3604(4)
Z	4	4	4
$D_{calc.}$ (mg m^{-3})	2.984	3.147	2.852
Crystal size (mm)	$0.12 \times 0.10 \times 0.10$	$0.20 \times 0.16 \times 0.07$	$0.25 \times 0.23 \times 0.19$
Crystal habit	Dark blue block	Black plate	Black block
$F(000)$	2500	2432	2800
μ (mm^{-1})	16.931	18.201	14.998
Max/min relative transmission	—	0.194, 0.086	1.000, 0.572
Data collection range (°)	$2.02 < \theta < 24.51$	$2.22 < \theta < 25.78$	$2.66 < \theta < 27.51$
Index ranges	$-15 \le h \le 15$, $-23 \le k \le 22$, $-15 \le l \le 15$	$-22 \le h \le 19$, $-16 \le k \le 14$, $-14 \le l \le 14$	$-22 \le h \le 5$, $0 \le k \le 15$, $0 \le l \le 22$
Reflections measured	15518	13709	5287
Independent reflections	4968 ($R_{int} = 0.070$)	2815 ($R_{int} = 0.0858$)	4010 ($R_{int} = 0.0429$)
Parameters, restraints	205, 16	205, 0	444, 373
wR_2(all data)[a]	0.197	0.0777	0.1154
x, y[a]	0.0721, 285.15	0.0279, 0	0.0673, 0
$R_1[I > 2\sigma(I)]$[a]	0.0785	0.0345	0.0465
Observed reflections	4229	2574	3484
Goodness-of-fit on F^2 (all data)[a]	1.147	1.065	1.029
Extinction coefficient	0.00130(10)	0.0030(2)	—
Maximum shift/σ	0.001	<0.001	0.004
Peak, hole in final difference map (e Å^{-3})	2.057, −3.511	1.536, −2.129	2.822, −3.586
Absolute structure parameter	—	—	−0.013(13)

[a] $R_1 = \Sigma \| F_o | - | F_c \| / \Sigma | F_o |$, $wR_2 = [\Sigma w((F_o^2 - F_c^2)^2 | \Sigma w F_o^4]^{\frac{1}{2}}$, $w = 1/[\sigma^2(F_o)^2 + (xP)^2 + yP]$, $P = (F_o^2 + 2F_c^2)/3$, where x and y are constants adjusted by the program; Goodness-of-fit $= [\Sigma[w(F_o^2 - F_o^2)^2]/(n-p)]^{1/2}$ where n is the number of reflections and p the number of parameters.

3.2. Preparation of [Os$_4$Rh(μ-H)$_3$(MeC=NH)(CO)$_{11}$(η^5-Cp)] **4**, [Os$_4$Rh(μ-H)$_2$(CO)$_{13}$(η^5-Cp*)] **5** and [Os$_4$Rh$_2$(μ-H)$_2$(CO)$_{11}$(η^5-Cp*)$_2$] **6***

An excess of [Rh(η^5-Cp*)(MeCN)$_3$][BF$_4$]$_2$ **3** (16 mg, 0.03 mmol) was added to a dichloromethane solution (20 ml) of the dianion [Os$_4$H$_4$(CO)$_{11}$]$^{2-}$ **2** with stirring. There was an immediate colour change from orange to blue/violet, and the solution was stirred for a further 20 min until the complete consumption of the starting material was achieved, as confirmed from the IR spectrum. The solution was filtered through celite and the filtrate condensed to a minimum volume under reduced pressure. The crude residue was purified by TLC using 40:60 CH_2Cl_2:hexane as eluent. In this method, the isolation of the products **4–6** depended on the initial addition of K/Ph_2CO to **1**. In separate reactions, in the presence of a minimum amount of K/Ph_2CO, mainly the starting material, with a 2% yield of the blue cluster [Os$_4$Rh(μ-H)$_3$(MeC=NH)(CO)$_{11}$(η^5-Cp*)] **4** is produced. Careful reduction of **1** with additional quantities of K/Ph_2CO affords the two clusters [Os$_4$Rh(μ-H)$_2$(CO)$_{13}$(η^5-Cp*)] **5** and [Os$_4$Rh$_2$(μ-H)$_2$(CO)$_{11}$(η^5-Cp*)$_2$] **6** in 10 and 2% yields, respectively. The yield of **6** can be increased to 12% by the addition of excess K/Ph_2CO to the dianion **2** and the subsequent reaction with **3**.

Microanalysis: **4**, found C, 21.17; H, 1.97. Calc. for $C_{23}H_{22}NO_{11}Os_4Rh$, C, 20.43; H, 1.64; **5**, found C, 19.98; H, 1.07. Calc. for $C_{23}H_{17}O_{13}Os_4Rh$, C, 20.23; H, 1.26; **6**, found C, 24.88, H, 1.78. Calc. for $C_{31}H_{32}O_{11}Os_4Rh_2$, C, 24.06; H, 2.08.

*3.3. Crystal structure determinations for **4**, **5** and **6***

Suitable single crystals for the three compounds were

mounted on glass fibres using a perfluoropolyether oil which freezes at reduced temperatures [26] and holds the crystal static in the X-ray beam. Two data sets for **4** were recorded on a Rigaku R-Axis IIc image plate diffractometer, one of $60 \times 3°$ oscillation frames, 8 min exposure, then the crystal was rotated through 90° about an axis 45° to the vertical and the second set of $30 \times 3°$ oscillation frames, 8 min exposure, were measured. An empirical absorption correction was achieved by merging equivalent reflections and by interframe scaling. Data for **5** was recorded using the Bruker AXS SMART CCD area-detector diffractometer, on the single crystal diffraction station 9.8, at the Daresbury Laboratory Synchrotron Radiation Source. Intensities were integrated [27] from several series of exposures, each exposure covering 0.15° in ω, with an exposure time of 0.2 s, and the total data set being more than a hemisphere. A semi-empirical absorption correction was applied on multiple and symmetry-equivalent measurements [28]. The data for **6** was recorded on a Rigaku AFC5R four-circle diffractometer using $\omega/2\theta$ scans. Semi-empirical absorption corrections based on ψ-scans were applied [29]. Each diffractometer was equipped with an Oxford cryostream crystal cooling device. Details of crystal data, data collection, and structure solution and refinement are summarised in Table 5. The structures were solved by direct methods (metal atom positions) [28,30] and by subsequent Fourier difference syntheses, and were refined by full-matrix least squares [31] on F^2. For **4** only the metal atoms were refined with anisotropic displacement parameters, while for **5** and **6** all non-hydrogen atoms were refined anisotropically. In the structure of **4** half a molecule of benzene was located in the crystal lattice, this was refined with half occupancy and was constrained to be a regular hexagon. Additional restraints were applied to the displacement parameters for the C and O atoms in the structure of **6** to improve the refinement. For all three structures the hydride H-atoms were not located in the Fourier difference maps but their positions were located using potential energy calculations [12]; their positions were included in the final structure factor calculation, but they were not refined. The pentamethyl cyclopentadienyl H-atoms were placed in idealised positions and allowed to ride on the relevant carbon atom; H-atoms were refined with isotropic displacement parameters with values of 1.5 that of the C-atoms to which they were attached. The methyl H-atoms on C(44) and the H-atom on N(1), in **4**, were also placed in idealised positions and allowed to ride on the heavier atom. For each structure, in the final cycles of refinement, a weighting scheme of the form $w = 1/[\sigma^2(F_o)^2 + (xP)^2 + yP]$ where $P = (F_o^2 + 2F_c^2)/3$ was introduced, and this resulted in a relatively flat analysis of variance. Atomic coordinates, displacement parameters, and bond lengths and angles for each of the structures have been deposited at the Cambridge crystallographic data centre (CCDC).

Acknowledgements

We thank the EPSRC for financial support for the purchase of instrumentation and for fellowships (to N.F. and S.J.T) and for a studentship (to G.P.S). We gratefully acknowledge the financial support of the Cambridge Commonwealth Trust and the United Kingdom Committee of Vice Chancellors and Principals (to S.N.), the Cambridge crystallographic data centre (to G.P.S.), and the CCLRC (to W.C.). A.M.M.C. wishes to thank the Spanish Ministry of Education and the British Council for a grant and for study leave. We are grateful to Johnson Matthey for a generous loan of osmium and rhodium salts.

References

[1] E.L. Muetterties, T.N. Rhodin, E. Band, C.F. Bruker, W.R. Pretzer, Chem. Rev. 79 (1979) 91.
[2] (a) W.E. Geiger, N.G. Connelly, Adv. Organomet. Chem. 24 (1987) 87. (b) P. Lemoine, Coord. Chem. Rev. 83 (1988) 169. (c) P. Zanello, Coord. Chem. Rev. 87 (1988) 1.
[3] (a) G. Schmid (Ed.), Clusters and Colloids, VCH Weinheim, Germany (1994). (b) U. Simon, G. Schön, G. Schmid, Angew. Chem. Int. Ed. Engl. 32 (1993) 250.
[4] (a) B.F.G. Johnson, J. Organomet. Chem. 475 (1994) 31. (b) D. Braga, P.J. Dyson, F. Grepioni, B.F.G. Johnson, Chem. Rev. 94 (1994) 1585.
[5] (a) H. Wadepohl, Angew. Chem. Int. Ed. Engl. 31 (1992) 247. (b) J. Lewis, C.K. Li, P.R. Raithby, W.T. Wong, J. Chem. Soc. Dalton Trans. (1993) 999. (c) J. Lewis, C.A. Morewood, P.R. Raithby, M.C. Ramirez de Arellano, J. Chem. Soc. Dalton Trans. (1996) 4509.
[6] D.S. Shephard, T. Maschmeyer, B.F.G. Johnson, J.M. Thomas, G. Sankar, D. Ozkaya, W. Zhou, R.D. Oldroyd, R.G. Bell, Angew. Chem. Int. Ed. Engl. 36 (1997) 2242.
[7] P.R. Raithby, G.P. Shields, Polyhedron (1998) in press.
[8] S.Y.W. Hung, W.T. Wong, Chem. Commun. (1997) 2099.
[9] R.K. Henderson, P.A. Jackson, B.F.G. Johnson, J. Lewis, Inorg. Chim. Acta 198–200 (1992) 393.
[10] J.E. Davies, S. Nahar, P.R. Raithby, G.P. Shields, J. Chem. Soc. Dalton Trans. (1997) 13.
[11] J. Lewis, C.K. Li, P.R. Raithby, M.C. Ramirez de Arellano, W.T. Wong, J. Chem. Soc. Dalton Trans. (1993) 1359.
[12] A.G. Orpen, J. Chem. Soc. Dalton Trans (1980) 2509.
[13] M. McPartlin, W.J.H. Nelson, J. Chem. Soc. Dalton Trans. (1986) 1557.
[14] R.D. Adams, D.A. Katahira, L.W. Wang, J. Organomet. Chem. 296 (1985) 209.
[15] M.A. Andrews, G. van Buskirk, C.B. Knobler, H.D. Kaesz, J. Am. Chem. Soc. 101 (1979) 7245.
[16] A. Colombie, D.A. McCarthy, J. Krause, L.Y. Hsu, W.L. Hsu, D.Y. Jan, S.G. Shore, J. Organomet. Chem. 383 (1990) 421.
[17] (a) G.R. John, B.F.G. Johnson, J. Lewis, W.J. Nelson, M. McPartlin, J. Organomet. Chem. 171 (1979) C14. (b) J.J. Guy, G.M. Sheldrick, Acta Crystallogr. Sect. B 34 (1978) 1725.

[18] B.E. Mann, B.F. Taylor, ^{13}C-NMR Data for Organometallic Compounds, Academic Press, London, 1981.
[19] W.E. Lindsell, C.B. Knobler, H.D. Kaesz, J. Organomet. Chem. 296 (1985) 209.
[20] R. Mason, K.M. Thomas, D.M.P. Mingos, J. Am. Chem. Soc. 95 (1973) 3802.
[21] J. Lewis, C.K. Li, M.R.A. Al-Mandhary, P.R. Raithby, J. Chem. Soc. Dalton Trans. (1993) 1915.
[22] J. Lewis, C.K. Li, C.A. Morewood, M.C. Ramirez de Arellano, P.R. Raithby, W.T. Wong, J. Chem. Soc. Dalton Trans. (1994) 2159.
[23] S.A.R. Knox, J.W. Knoepke, M.A. Andrews, H.D. Kaesz, J. Am. Chem. Soc. 97 (1975) 3942.
[24] M.R.A. Al-Mandhary, Ph. D. Thesis, University of Cambridge (1994).
[25] C. White, A. Yates, P.M. Maitlis, Inorg. Synth. 29 (1992) 228.
[26] D. Stalke, T. Kottke, J. Appl. Crystallogr. 26 (1993) 615.
[27] SMART (Control) and SAINT (Integration) Software, Bruker AXS, Madison, WI, 1994.
[28] G.M. Sheldrick, SHELXTL version 5 and SADABS (corrections for area detector data), Bruker AXS, Madison, WI, 1995 and 1997.
[29] (a) TEXSAN, Version 1.7–1, Molecular Structure Corporation, The Woodlands, TX, 1985, 1992, 1995. (b) A.C.T. North, D.C. Phillips, F.S. Mathews, Acta. Crystallogr. Sect. A 24 (1968) 351.
[30] A. Altomare, G. Cascarano, C. Giacavazzo, A. Guagliardi, M.C. Burla, G. Polidori, M. Camalli, J. Appl. Crystallogr. 27 (1994) 435.
[31] G.M. Sheldrick, SHELXL 93, Program for Crystal Structure Refinement, University of Göttingen, Göttingen, 1993.